Wavelets Application in Acoustic Emission Signal Detection of Wire Related Events in Pipeline

Ran Wu[1], Zaiyi Liao[2], Lian Zhao[1] and Xiangjie Kong[3]
1 Dept. of Elec. & Comp. Eng., Ryerson University, Toronto, ON, Canada.
2 Dept. of Architecture, Ryerson University, Toronto, ON, Canada.
3 Pressure Pipe Inspection Company Ltd., Mississauga, ON, Canada.

ABSTRACT

As a popular nondestructive test, acoustic emission (AE) testing has been widely used in many physical and engineering fields such as leak detection and pipeline inspection. Among those applied AE tests, a common problem is to extract the physical features of the ideal events, so as to detect similar signals. In acoustic signal processing, those features can be represented as joint time-frequency distribution. However, classical signal processing methods only give global information on either time or frequency domain, while local information is lost. Although the short-time Fourier transform (STFT) is developed to analyze time and frequency details simultaneously, it can only achieve limited precision. Wavelet transform is a time-scale-frequency technique with adaptable precision, which makes better feature extraction and detail detection. This paper is an application of wavelet transform in acoustic emission signal detection where strong noise exists. Developed for industrial applications, the techniques presented are both accurate and computationally implemental for embedded systems. In addition, STFT is compared with wavelet transform to show the advantages of wavelet transforms in this particular application.

SOMMAIRE

Étant aujourd'hui l'un des plus populaires essais non destructifs, le contrôle par émissions acoustiques (EA) est utilisé dans divers domaines, relevant tant de la physique que de l'ingénierie. On les retrouve principalement pour la détection des fuites, ou encore pour l'inspection des pipelines. Dans les différentes applications, on retrouve un problème commun, celui d'obtenir les caractéristiques physiques des événements idéaux afin de détecter les signaux semblables. Dans le traitement des signaux acoustiques, ces caractéristiques peuvent être représentées simultanément dans le domaine du temps et de la fréquence. Cependant, la méthode classique du traitement des signaux donne seulement des informations générales sur ces domaines, mais ne fourni pas une analyse détaillée. En effet, bien que la transformé de Fourier à court terme a été développé pour analyser le temps et la fréquence simultanément, elle dispose d'une précision limitée. La transformé de Wavelet est une méthode de type temps-fréquence-échelle, avec une précision adaptable, qui permet d'obtenir un relevé plus précis et de meilleure qualité. Ce dossier présente une application de la transformé de Wavelet pour la détection d'une émission acoustique qui contenant beaucoup de perturbations. Développées pour l'industrie, les techniques présentées sont à la fois précises et facilement applicables aux systèmes intégrés. Afin de faire ressortir les avantages de la transformé de Wavelet dans ce type d'application, vous trouverez une comparaison entre cette dernière et la méthode de Fourier à court terme.

1 INTRODUCTION

Acoustic Emission (AE) testing has been widely used in physical and architecture fields due to its efficiency, reliability and lower operation costs. In steel pipelines, when a present defect expands, tension energy is released, and an acoustic signal is generated [1]. AE techniques are used to observe and monitor these events. Although some events occur before monitoring, or are too weak to be detected during inspection, various events occur due to temperature, pressure, physical defect development and environmental conditions so that they become detectable. Previous studies showed that the

amplitude of AE signal is proportional to the released energy [2], and the frequency distribution is related with the size of the defect [3]. For instance, in leak detection of a pipeline, the AE signal detected from larger leak hole contains more low frequency components. This can be explained that larger hole creates smaller pressure, which results in lower frequency components.

The AE events that occur in pipeline usually create two types of signals: one is a mechanical wave which propagates along the steel wire in the pipe at high frequency (above 100 kHz), another is a low frequency wave (about 30 kHz) that propagates through the medium (gas or liquid) inside the pipe. Stulen and Muravev showed in their research [1,4]that the attenuation of the waves has a square relationship with their frequency, and the coefficient of this relationship is distinguished by the particular medium. Observed values for attenuation (in dB/ft) in several gases and water are $4.9 \times 10^{-11} f^2$ and $7.8 \times 10^{-14} f^2$, respectively, where f is the frequency. Therefore, AE signals propagating through the steel wire attenuate very quickly because the frequency is high. However, those low frequency waves that propagate in the medium can be detected even at sites hundreds of meters away from the original signals. In addition, this kind of wave interacts with the pipe wall so that it can be detected by sensors mounted outside of the pipe.

For AE signal detection and feature extraction, many acoustic signal processing methods have been used. Classical frequency analysis [3]gives very rough information about the signal, such as global spectrum, frequency peaks and SNR, which makes the detection work ambiguous. In fact, time variant features that can be depicted by changing signal frequency components with time, is the main character of acoustic signals. This is similar to music composition. Each musical tone is the combination of certain frequency bands, and different tones arrive at different times to make the music. Therefore, we need to know the arrival time and location of those frequency components in the time domain, in order to discriminate different AE signals and detect the right events. Therefore, in the time-frequency plane, these local details are much more important than global information.

This requirement cannot be satisfied by classical Fourier transform. To solve this time-frequency problem, Short-time Fourier transform (STFT) was applied to signal processing [5]. STFT uses small windows to localize a signal in the time domain, and then applies Fourier transform to get the frequency distribution only in this window. However, this STFT window, or atom, has certain size and precision restrictions, which locks the time-frequency at certain resolution level. The wavelet transform, which was first created in seismology, was introduced to signal processing to solve this multi-resolution problem [6].

This paper presents part of the research that aims to detect the real AE events accompanied by strong noise. Both STFT and Wavelet transform are implemented to thoroughly analyze the time-frequency occurrence of both AE signal and noise. After comparison, Wavelet transform techniques are chosen for the final application. Using features extracted in wavelet domain, experiments are carried out over a large number of industrial data.

The remaining of the paper is organized as the following: Section 2 reviews the current applied technology, gives the physical condition and environment for the AE signal detection, as well as extracted features. Section 3 provides the basis of wavelet transform and STFT. Section 4 analyzes these two methods in detail. Section 5 is experiment results of the proposed method. Section 6 concludes the paper.

2 CURRENT APPLIED TECHNOLOGY

In industry, people are using AE testing for detecting wire related events (WRE) in pipelines. Signals from the pipelines provide the observed data for this research. The environment and preconditions are described below.

2.1 Physics conditions

The tested portion of the pipeline was constructed in 1975 with Lined Cylinder Pre-stressed Concrete Cylinder Pipe (PCCP)[7], as shown in Fig. 1. The PCCP is constructed by first casting a steel cylinder outside of a concrete core, pre-stressed wire around it. This high strength wire is de-

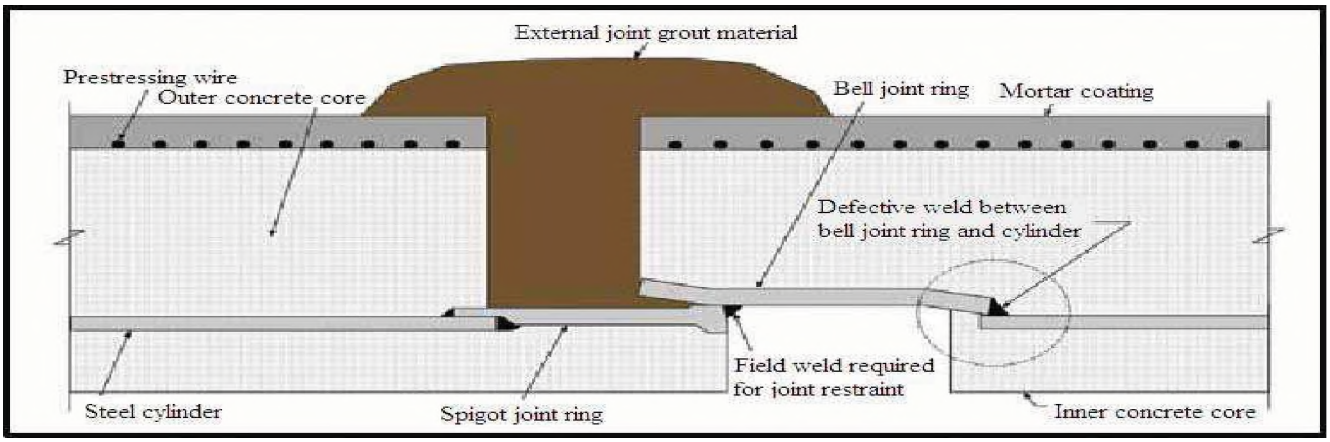

Figure 1: Lined cylinder PCCP.

signed to force the core tighter, and is then coated with a mortar coating, so as to provide corrosion protection to the wire. Therefore, this pre-stressing wire is the key component of the PCCP, and the main purpose of AE testing here is to take precautions against the corrosion and breakage of the wire. Once the wire break or split occurs, the tension energy embedded in the wires will be released, and acoustic waves will be generated. After propagating through the medium inside the pipe, these waves can be detected and recorded by acoustic sensors as long as the amplitude of the signal is higher than the defined threshold.

In current practice, two types of sensors have been used to detect WRE signals: hydrophone and accelerometer. Hydrophones are constructed of ceramic materials and can detect acoustic signals by sensing the vibration that is propagated through water. Hydrophones are installed through valves into the water column inside the pipeline, as shown in Fig. 2(a). Accelerometers are installed on the surface of the pipeline, as shown in Fig. 2(b). Incentive to use accelerometers in AE testing is to assist hydrophones, as hydrophones are more sensitive than accelerometers. They are also used in the case of empty pipelines.

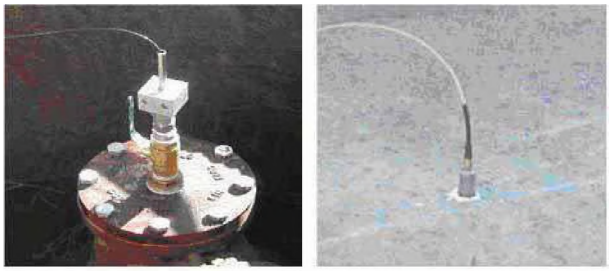

Figure 2: (a) Hydrophone sensor. (b) Accelerometer sensor.

Once the AE event occurs, the signal will propagate both ways along the pipeline, and may be detected by the closest pair of sensors. Sometimes if the amplitude is large enough, the signal might be detected by the third or the forth sensor. As studied in [1], the detected result is reliable with sensor spacing at 262 meters distance, and this can vary according to landscape, temperature, pipe structure, . Therefore, an ideal WRE signal should be detected by two sensors closest to it, and the arrival time difference can be used to localize the defect's position. If the signal is only picked up by one sensor, then the position cannot be accurately localized, and the recorded data will not be considered as useful.

2.2 Acoustic signal features

Fig. 3 is an example of AE event signal detected by the closest two sites: site 1 is 68.6 meters from the event where the sensor is a hydrophone; site 2 is 90.8 meters from the event where the sensor is an accelerometer. Some features of this WRE signal are shown in Fig. 4. Figs. 4(a), 4(c), and 4(e) show the time domain, frequency domain and the Gabor time-

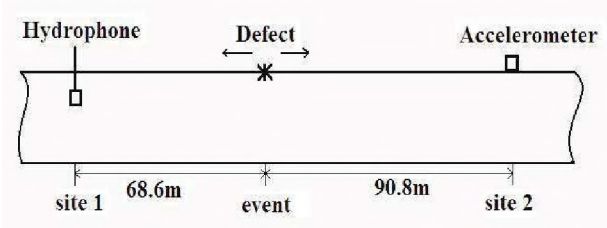

Figure 3: An AE event detected by two sites.

frequency domain respectively, of the recorded signal at site 1; Figs. 4(b), 4(d), and 4(f) provide the corresponding information of the recorded signal at site 2 [4].

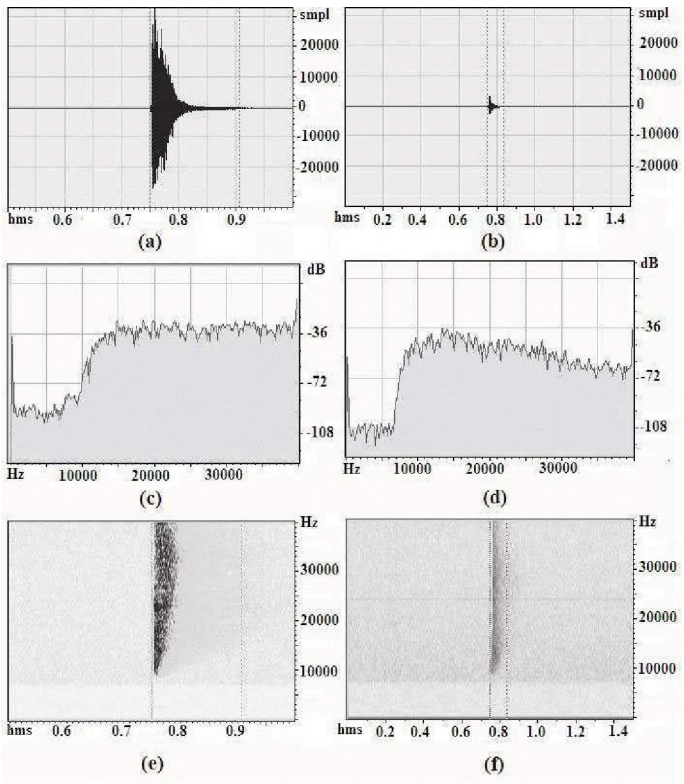

Figure 4: (a), (c) and (e) are the time domain, frequency domain, and Gabor transform, respectively, of the signal recorded by Hydrophone; (b), (d) and (f) represent the same signal recorded by Accelerometer.

Figs. 4(a) and 4(b) clearly show the signal amplitude recorded by the hydrophone is much larger than that recorded by the accelerometer. In the Gabor transform, Figs. 4(e) and 4(f), larger amplitude and energy intensity in the signal will make the color darker. From the time-frequency analysis shown in Figs. 4(e) and 4(f), the signal-to-noise ratio (SNR) of the left one is much higher than the right one, because the left signal has greater energy. Although the noise level of these two signals are almost the same (shown as the gray level of the background), the larger energy in the left signal results in a larger SNR.

Some observations can be drawn as follows:

- In the time domain [Figs. 4(a), 4(b)]:

The duration of the signal is usually less than 0.05 seconds. The intensity of the signal should be much larger than the background. while in frequency domain (Figs. 4(c), 4(d)) this corresponds to the spectrum amplitude of the signal, and in the time-frequency Gabor window (Figs. 4(e), 4(f)) it means the color of the signal should be much darker than the background.

- In the frequency domain [Figs. 4(c), 4(d)]:

These figures show the "real-time" spectrum of the signal. This WRE signal has the following unit step form, as shown in Fig. 5(a), where the solid line is the spectrum shape at the beginning time , and the dashed line is the spectrum shape at the ending time.

For the beginning of the signal in time axis: 7 kHz is the start frequency of all sounds (mostly background), 12 kHz is the start frequency of the WRE signal, and the highest frequency is above 40 kHz.

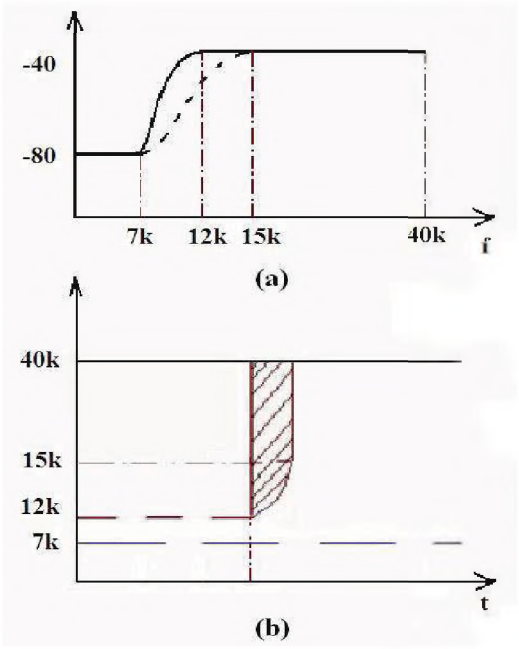

Figure 5: (a) frequency response of an WRE signal: solid line is the spectrum shape at the beginning time; dashed line is the spectrum shape at the ending time. (b) Gabor windowed time-frequency distribution of an WRE signal.

For the ending of the signal in time axis: 15 kHz is the start frequency of WRE signal, the highest is above 40 kHz. These parameters can be different in particular situations, while the shape should be similar. As shown in Figs. 4(c) and 4(d), the high frequency decrease greatly due to the attenuation of signal propagating through the pipeline to the accelerometers.

- In the time-frequency Gabor window [Figs. 4(e), 4(f)]:

As shown in those Gabor figures, the power density starts at above 7 kHz, while lower than 7 kHz the color is all white, which means that there is no frequency component in this part. From the beginning of the signal at 0.75 seconds until the ending at 0.80 seconds, the shape of the power density is like a vertical downward knife, as shown in Fig. 5(b). This knife shape is also referred to "J" shape in the industry. The peak of the knife is the beginning of the signal with 12 kHz frequency, which decreases earliest and at the fastest speed; hence, at the ending time, 15 kHz becomes the start frequency. In addition, the intensity of the signal from 15 kHz to 40 kHz is almost uniformly distributed, and this feature makes the two vertical parallel lines.

3 APPLICATION OF WAVELETS COMPARED WITH STFT

3.1 Basis of STFT

Fourier transform is defined to obtain the frequency distribution of a signal when the signal is transformed through the whole time domain. In addition, the stationarity of the signal is also required. In other words, the spectrum information of the signal has been averaged through the whole time domain, which results in the loss of real-time spectrum occurrence [8].

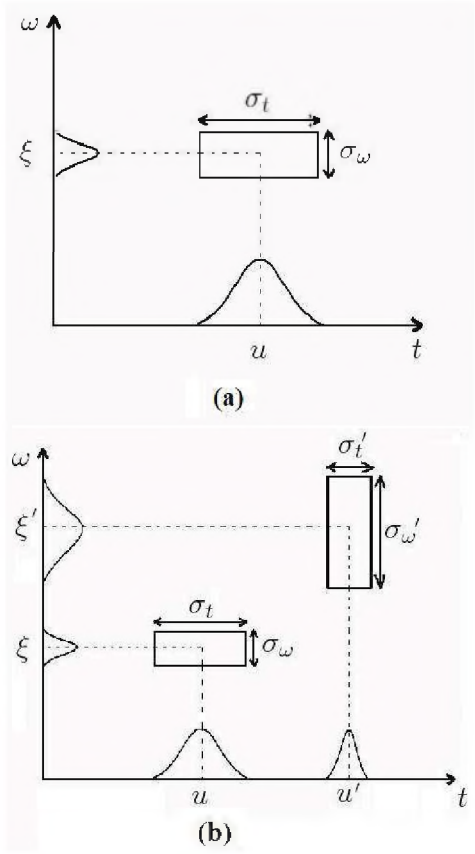

Figure 6: (a) the STFT window. (b) the graphical interpretation.

Short-Time Fourier transform (STFT) was introduced by Gabor [6]to compensate the limitation of classical Fourier transform and it provides an original joint time-frequency method. It uses a measuring window to restrict the Fourier transform in a limited time range and then obtain the spectrum on this time range. As Fig. 1(a) shows, this real and symmetric window $g(t)$ is delayed by u on time domain, and modulated by the frequency ξ [9]:

$$g_{u,\xi}(t) = e^{i\xi t} g(t-u) \tag{1}$$

The STFT of a signal $f(t) \in L^2(\mathcal{R})$ is:

$$S\{f(u,\xi)\} = < f, g_{u,\xi} > = \int_{-\infty}^{\infty} f(t) g(t-u) e^{-i\xi t} dt \tag{2}$$

where S stands for applying STFT to $f(t)$ with the (u,ξ) window, $< f, g_{u,\xi} >$ is the inner product of $f(t)$ and $g_{u,\xi}(t)$, and $L^2(\mathcal{R})$ is the whole function space. Therefore, the multiplication by $g(t-u)$ localizes the Fourier integral of $f(t)$ in the neighborhood of $t = u$, as shown in Fig. 1(a). In the figure, (u,ξ) is the center of the window in time-frequency domain, while σ_t and σ_ω are the width and length of the window, respectively. Therefore, after taking STFT, the energy of $f(t)$ is spread over both time interval $[u - \sigma_t/2, u + \sigma_t/2]$ and frequency interval $[\xi - \sigma_\omega/2, \xi + \sigma_\omega/2]$.

As discussed by Kaiser [10], STFT provides an inaccurate and inefficient method of time-frequency plane analysis, as it imposes a scale to do the localization. First, the inaccuracy comes from the aliasing of high and low frequency components, which actually do not fall into the frequency of the window [11]. Secondly, several window lengths must be selected and applied to determine the most appropriate one. Even though the appropriate window size has been determined, the provided time-frequency analysis is not only single resolution, but always averaged on both time and frequency dimensions.

STFT does not change the fact that the information in this time-frequency box is still averaged over both sides and that the information of sudden changes is lost. To satisfy the requirement of obtaining the occurrence of time-frequency information, Wavelet transform is introduced to perform this time-frequency-scale transformation, aiming at combining amplitude and spectrum decomposition together and as accurately as possible. In principle, when applied to the detection of discontinuities, short time phenomenon, and abrupt changes in a signal, Wavelet transform has better performance than other signal processing methods. It also provides higher resolution and better precision in presenting real-time changes of a signal's spectrum density function, thus, it is an essential way to characterize time-frequency structures [6]

3.2 Basis of wavelet transform

Wavelet transforms can be used to analyze non-stationary signals via decomposing and reconstructing them with wavelet basis or wavelet functions. There are two types of wavelet transform: Continuous Wavelet transform (CWT) and Discrete Wavelet transform (DWT). The term "wavelet basis" usually refers to orthogonal wavelets in the Hilbert space, while "wavelet function" generally represents either orthogonal or non-orthogonal wavelets [12]. In DWT, orthogonal wavelet basis is often applied to give the most compact representation of the signal. However, for time series analysis, CWT with non-orthogonal wavelet functions are recommended as it is highly redundant at large scales, and the wavelet spectrum is highly correlated [11]. In the proposed algorithm, CWT is also selected to apply the time-scale analysis for the time domain acoustic signals.

In CWT, a signal with finite energy is projected on a continuous collection of frequency bands, which compose the whole function space $L^2(\mathcal{R})$. The wavelet functions are the scaled shifts of one generating function $\psi_0(t) \in L^2(\mathcal{R})$, which is a continuous function in both the time domain and the frequency domain called the mother wavelet. These wavelet functions are given as:

$$\psi(t) = \frac{1}{\sqrt{a}} \psi_0 \left(\frac{t-b}{a} \right) \tag{3}$$

where a is a positive scale factor and b can be any real number that defines the shift. The normalization factor $\frac{1}{\sqrt{a}}$ is introduced to ensure the wavelet function have unit energy at each sale a.

CWT uses these wavelet functions to transfer time series into a time-scale wavelet domain, which provides a very detailed localization on both time t and scale a directions. Mathematically, it is defined as the convolution of the signal $f(t)$ with chosen wavelet functions [13]:

$$W_f(a,b) = \frac{1}{\sqrt{a}} \int_{-\infty}^{\infty} f(t) \psi_0^* \left(\frac{t-b}{a} \right) dt \tag{4}$$

where W_f represents the wavelet transform of $f(t)$, and '$*$' donates the complex conjugation operation. Valens also emphasized in his article [13]that it is important the wavelet functions are not specified in this mathematical wavelet frame, which is a clear ridge between wavelet transform and other transforms including Fourier transform. It is essential that wavelet transform designed a framework in which one can design wavelets for their own properties.

3.3 Comparison of CWT and Fourier transform

Compare equation (4) with continuous Fourier transform:

$$F_f(\omega) = \int_{-\infty}^{\infty} f(t) e^{-j\omega t} dt \tag{5}$$

It is apparent that Fourier transform is a specialized form of wavelet by substituting the wavelet functions with infinite and periodical sine and cosine waves. If we only take the wave in one period as the wavelet function (similar to what STFT does), then the period can be considered as the scale factor, as both of these two methods are sampling and quantizing signals so as to decompose them. As "period" in Fourier transform and "scale" in wavelet transform are proportional,

frequency and scale are inversely proportional to each other. That is, high frequency components refer to small scales in wavelet domain, and both of them represent small details in the signal.

When facing the non-localizable problem of Fourier transform, researchers introduced STFT to impose the localization grid onto the signal. Unfortunately, this method leads to a confusing way of explaining frequency components in the time-frequency domain, as we discussed at the very beginning of this section. The particular window in STFT is a scale factor. However, if its size is constant, it can only represent the averaged frequency components inside the window, but not the real frequency components. This is why Kaiser regards it as inaccurate in building up the time-frequency analysis [10].

Therefore, compared to regarding wavelet transform as an extension of Fourier transform, it is more appropriate to state that Fourier transform is a particular case of wavelet transform, as wavelet transform is not only a transform but a framework for researchers to fill in their own wishes.

3.4 Applying CWT to discrete time sequence

Although CWT has been chosen for the time series analysis, a discrete form of CWT is needed for discrete time sequence and for the computational implementation. We can make the assumption of a time sequence, $x(n)$, with equal time step Δ_t and $n = 0, 1, \cdots, N-1$. Assume the wavelet function is given as $\psi_0(t)$, where t is a non-dimensional time parameter to form the function. Take Morlet wavelet for example (details will be provided in next section):

$$\psi_0(t) = \pi^{-\frac{1}{4}} e^{j\omega_0 t} e^{-\frac{t^2}{2}} \tag{6}$$

This is a complex sine wave modulated by a Gaussian function, and ω_0 donates the non-dimensional frequency parameter. Then wavelet transform in (4) can be written as [11]:

$$W_f(a,b) = \sqrt{\frac{\Delta_t}{a}} \sum_{n=0}^{N-1} \left\{ x(n) \psi_0^* \left[\frac{(n-b)\Delta_t}{a} \right] \right\} \tag{7}$$

In this equation, it can be seen that the convolution should be done for N times for each scale a. Thus, we can use discrete Fourier transform (DFT) to complete these N times convolution simultaneously. The DFT is calculated as:

$$\hat{X_k} = \frac{1}{N} \sum_{n=0}^{N-1} x(n) e^{-\frac{2\pi j k n}{N}} \tag{8}$$

According to Fourier's properties, convolution in time domain corresponds to multiplication in frequency domain. Hence equation (7) can be written as:

$$W_f(a,b) = FFT^{-1} \left\{ \sqrt{\frac{2\pi a}{\Delta_t}} \sum_{n=0}^{N-1} \left[\hat{X_k} \hat{\Psi_0}^*(a\omega_k) e^{i\omega_k b \Delta_t} \right] \right\} \tag{9}$$

where ω_k is the angular frequency defined as:

$$\omega_k = \begin{cases} \frac{2\pi k}{N\Delta_t}, & k \leq \frac{N}{2} \\ -\frac{2\pi k}{N\Delta_t}, & k > \frac{N}{2} \end{cases} \tag{10}$$

3.5 Morlet wavelet

There are several known mother wavelets in CWT, for example, Morlet, Meyer and Mexican hat wavelet. All the mother wavelets must satisfy the conditions of zero mean and unit energy, respectively given as:

$$\begin{aligned} \int_{-\infty}^{\infty} \psi(t) dt &= 0 \\ \int_{-\infty}^{\infty} |\psi(t)|^2 dt &= 1 \end{aligned} \tag{11}$$

Among these wavelet functions, Morlet wavelet is the earliest wavelet function used in CWT. It is a complex wavelet that contains the real part and the imaginary part, represented by a solid wave and a dashed wave respectively in Fig.7(a). The frequency domain representation of Morlet is a single symmetric Gaussian peak, as shown in Fig.7(b), which provides a better localization result in both time and frequency domain than the sharp peak of a sinusoid.

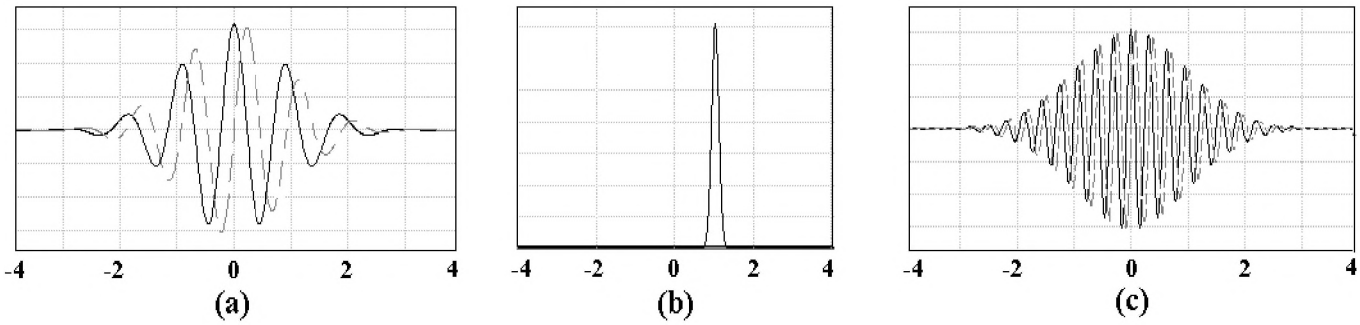

Figure 7: (a) Morlet wavelet with $\omega_0 = 6$. (b) spectrum of Morlet wavelet in (a). (c) Morlet wavelet with $\omega_0 = 20$.

In the Morlet wavelet equation (6), there is an admissibility condition of $\omega_0 > 5$. This ω_0 corresponds to the number of waves in Morlet. As shown in Figs. 7(a) and 7(c), the wave numbers are 6 and 20, respectively.

4 RESULTED ANALYSIS

4.1 Comparison of STFT and wavelet transform

In the CWT implementation, the Morlet wavelet has been chosen; and for the STFT illustration, the Gauss window is selected. The signals from industrial data are all '.wav' files with 1.5 seconds duration. In our experiment, all the signals are normalized to the same amplitude level in time domain. This means the amplitude of those accelerometer signals has been largely amplified. Furthermore, in both CWT and STFT computation, only the main part of the signal is processed, , the duration from $0.75s$ to $0.80s$ (in the following figures it is from 0 to 6, as there are 6000 samples). The pre-signal and post-signal noise has been removed to concentrate on feature extraction and to minimize the computational work.

4.1.1 Scale vs. frequency

When comparing wavelet transform with Fourier transform, it should be noted that frequency in Fourier transform and scale in wavelet transform are inversely proportional to each other. Hence, scale has a certain relationship with frequency. In [14], the following equation states this relationship especially for Morlet wavelet

$$a = \frac{b}{\omega} \tag{12}$$

where b is a constant, a is the scale parameter, and ω is the circular frequency of the signal.

Fig. 8 shows a typical WRE signal recorded by hydrophone, in both wavelet's time-scale distribution and STFT's time-frequency distribution, respectively. In addition, the 3D illustration of the wavelet domain is given to show the scale components clearly. The amplitude of the signal is described in red and blue colors. Generally, the color changing from blue to red implies the increased amplitude. Pure blue color represents only the background where no signal exists.

As shown in Fig. 8(b), in wavelet domain, the signal starts at scale 10, which corresponds to about 10 kHz in frequency domain in Fig. 8(c). It should be noted that the axis of scale a in Fig. 8(b) and frequency v in Fig. 8(c) are inversely distributed as explained before. The part of smaller than scale 2 in wavelet domain corresponds to above 30 kHz in STFT figures. This shows that high frequency components are highly compressed in wavelet domain due to Wavelet transform's characteristics. The part of larger than scale 8 corresponds to frequency lower than 12 kHz in STFT figures, and the details in this region have been significantly enhanced in wavelet domain.

4.1.2 Multi-resolution vs. single resolution

These compressing and enhancing properties make Wavelet transform more advanced than Fourier transforms such as STFT. Wavelet transform has multi-resolution for different scales. This property meets the need of our research appropriately. While for STFT, there is only one consistent resolution for the whole signal in time-frequency plane, thus the resolution of those frequency components cannot be distinguished for different uses. In this AE application, we would like to both enlarge low frequency components and compress high frequency components. These two objectives can be easily achieved using Wavelet transform rather than STFT. Because in STFT, different frequency components will be enlarged or shrunk together, as it has only one consistent resolution.

4.1.3 Detailed exhibition vs. averaged information

Except for above facts, the resolution of using STFT in AE signal processing is too low, and the details of the signal are wholly averaged over the STFT window. This means, if we want smaller unit length and more details in the frequency domain, the unit length in the time domain will be increased as the area of this time-frequency piece should keep the same. While for wavelet transform technique, the problem has been solved, as it is designed to exhibit the sharp discontinuities and fast changes. This is also shown in Figs. 8(a) and (b): in the time domain, there is a clear gap in the middle of the signal (white box framed), and in the wavelet domain this is apparently shown with the same gap length. However, in the STFT analysis of Fig. 8(c), the gap has been averaged that it is hard to notice. From this we can see that the unit time length in STFT is too large to detect the real-time changes of the amplitude, which results in losing signal features in the joint time-frequency occurrence.

4.2 Comparison of hydrophone and accelerometer

Fig. 10 compares the wavelet and STFT domain of a WRE signal recorded by accelerometer. As described before, this signal has certain differences with the hydrophone signal, in both amplitude and joint time-frequency structure.

As shown in Fig. 10, the overall amplitude of this accelerometer signal is smaller than previous signal in Fig. 8, although this signal is normalized. This is clearly shown in STFT figures, Fig. 10(c) and Fig. 8(c), due to STFT's low resolution and average of those larger-amplitude details. Moreover, the 3D meshing models of wavelet in Fig. 10(d) and Fig. 8(d) also illustrate this phenomenon. For the hydrophone's 3D model in Fig. 8(d), there are several red hilltops in the signal duration. While for the accelerometer in Fig. 10(d), there is only one clear peak.

Another feature here to distinguish accelerometer signals with hydrophone is the blank region (green box framed) around scale 2, which doesn't clearly appear in hydrophone's figures. This blank region corresponds to about $30 - 35$ kHz in frequency domain, which demonstrates the attenuation of high frequency in accelerometer's cases.

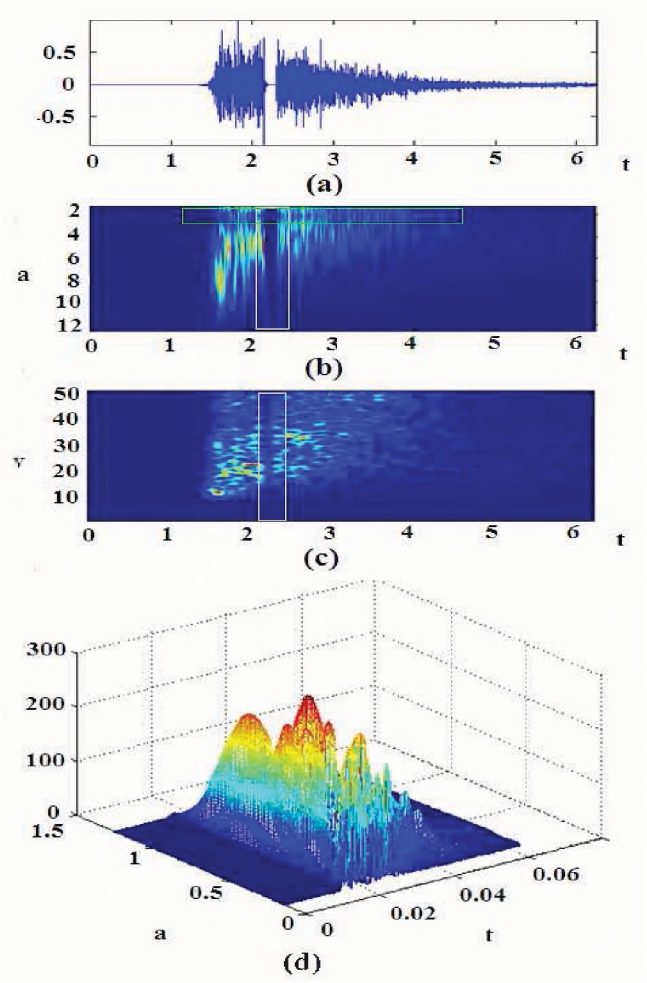

Figure 8: Transforms of a Hydrophone WRE signal: (a) time domain. (b) wavelet domain. (c) STFT for the signal. (d) 3D illustration of the wavelet domain.

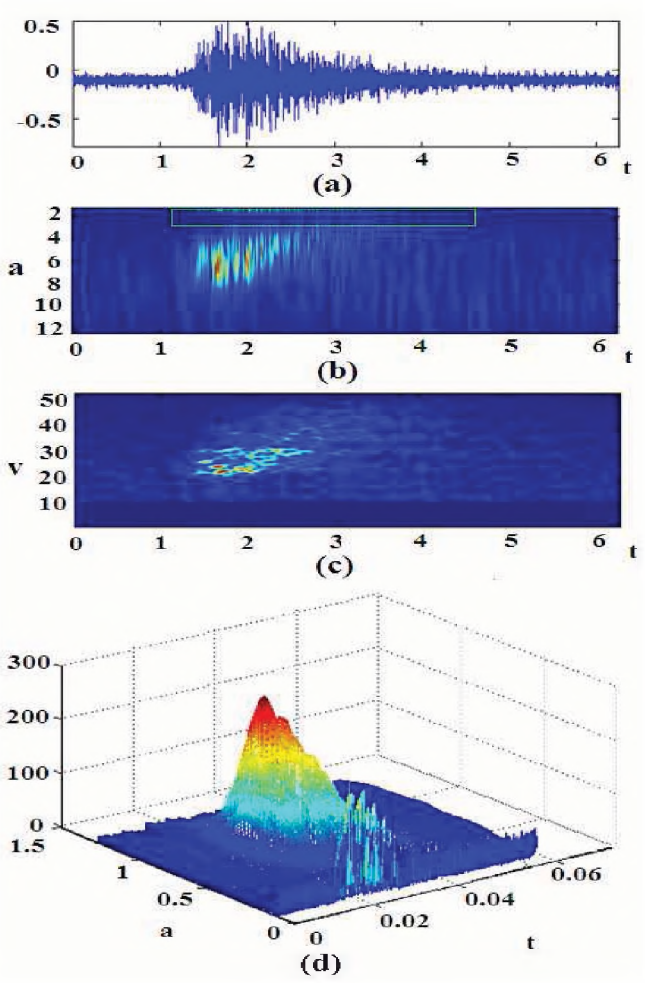

Figure 10: Transforms of a Accelerometer WRE signal: (a) time domain. (b) wavelet domain. (c) STFT for the signal. (d) 3D illustration of the wavelet domain.

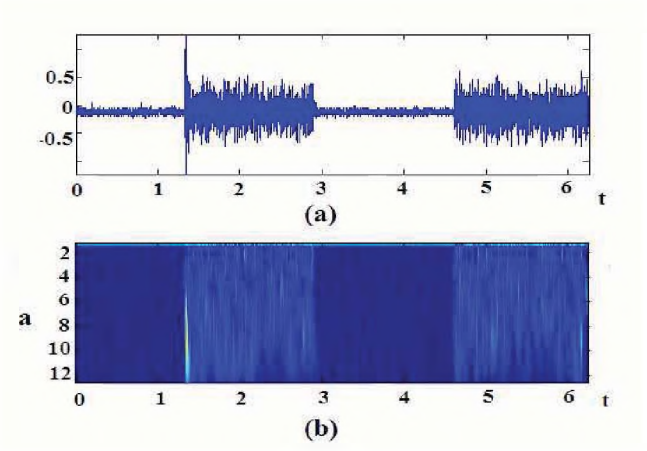

Figure 9: Wavelet transform of the first noise signal: (a) time domain. (b) wavelet domain shows very scattered density of noise signal 1.

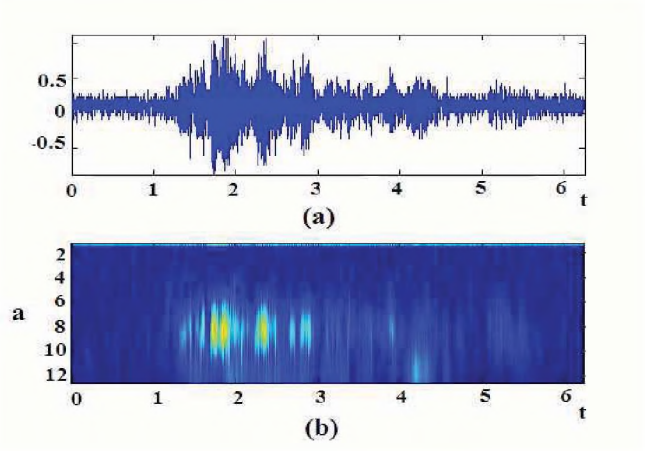

Figure 11: Wavelet transform of the second noise signal: (a) time domain. (b) wavelet domain shows large scale noise(low frequency) of noise signal 2.

4.3 Features of WRE signal in wavelet domain

This part deals with purpose of this research, which is to filter out most non-WRE signals and to detect the real WRE signals. Therefore, certain criteria should be set up as a dynamic filter. Before setting the criteria, features of ideal WRE signal should be summarized based on previous analysis. In addition, due to the different conditions of hydrophone and accelerometer, the features are distinguished according to different cases.

From the above analysis, the similar result obtained in section 2 can be concluded. However, due to Wavelet transform's high precision and enhancement of the abrupt changes in signal, we can see from the above figures that the large scale part, corresponding to low frequency component, decreases with time lapse almost linearly. This feature is important for the detection of real WRE signals. However, in the Gabor window mentioned in section 2, "the sharp of the knife", which describes the low frequency declining, does not seem to have this clear linear shape.

Figs. 9 and 11 exhibit two non-WRE data, which are typical noise signals with certain features: one is mess noise with scattered energy density; another is low-frequency noise, which locates much more in large scale part than in small scale part. These two types are the typical noise signals existing in the pipeline inspection.

From the plentiful industrial data, certain features of WRE signal have been concluded, which are also shown in Figs. 8 and 10:

- The energy should be concentrated in the main signal duration locating at 0.75s to 0.80s.
- Less than 20% of the energy lies in the location of scale $a > 8$, corresponding to low frequency region of $f < 12kHz$.
- More than 40% of the energy lies in the location between scale $2 < a < 6$, corresponding to median and high frequency region of $15kHz < f < 40kHz$.

In these three features, it is very important that the energy of real AE signal should be very condensed, which means most of the power should lie in the shown time band. The recorded data is most likely to be random noise if the ratio of power is too small, indicating that the energy is not concentrated around the certain spectrum. A large amount of noisy signals can be eliminated through pre-processing based on this feature. Wavelet analysis is not needed in this preprocessing.

Table 1 gives the parameters for above three features according to the results of bountiful tests. The given ratios are calculated as following:

$$\text{PDR} = \frac{\text{the energy of signal from 0.75s to 0.80s}}{\text{the energy of the whole signal}}$$

$$\text{LSR} = \frac{\text{the energy of signal in scale interval } a > 8}{\text{the energy of the whole signal}}$$

$$\text{SSR} = \frac{\text{the energy of signal in scale interval } 2 < a < 6}{\text{the energy of the whole signal}}$$

These parameters are chosen to be tolerant enough not to miss weak WRE signals, but still get rid of most noise data. It should be noticed that these features are distinguished for hydrophone and accelerometer, due to their different signal characteristics: the parameters chosen for hydrophone are more strict than accelerometer in all three features, as hydrophone signals have higher SNR and are easier to be detected.

Table 1: Threshold of Hydrophone(Hyd) and Accelerometer(ACC) WRE signals

	Hyd	ACC
Power-density-ratio(PDR)	4.85%	4.25%
Large-scale-ratio(LSR)	15%	22%
Small-scale-ratio(SSR)	40%	33%

5 IMPLEMENTATION AND EXPERIMENT RESULTS

As mentioned at the beginning, the purpose of this research is to filter out non-WRE signals and detect the real WRE signals. The experiment is carried out in two steps: first, get rid of the obvious non-WRE signals in order to save storage and reduce computational demand; secondly, detect the real WRE signals.

5.1 Implementation

The algorithms of both wavelet and STFT are implemented in Matlab 7.1 platform. The wavelet detection procedure is a four-step program, shown as following, where PDR, LSR and SSR refer to the ratios in Table 1:

1. Extract only the main part of the signal, which locates at 0.75 to 0.80 seconds in the recorded duration.
2. Calculate the power-density-ratio (PDR) of the extracted signal over the whole signal:
   If the ratio is larger than the threshold – consider as suspected WRE for further process;
   If the ratio is smaller than the threshold – obvious non-WRE, filter out.
3. Wavelet transform of the suspected WRE.
4. Calculate the scale ratio of transformed WRE:
   the large scale ratio (LSR) should be less than the threshold;
   the small scale ratio (SSR) should be greater than the threshold.

In these four steps, the first two steps aim to get rid of most obvious non-WRE data, and they achieve desirable results. The last two are not always satisfied due to the variety of WRE, and the wavelet features should be modified according to particular practical demands. As this is industrial application, the probability of miss detection should be as small as

possible. It is a compromised situation to sacrifice the detection accuracy. Therefore, in real implementation, for the forth step, satisfying either feature will be considered as suspected-WRE, so as to reduce the miss detection probability.

5.2 Computational complexity issue

As the method and algorithm will be fully implemented in embedded system for industrial installation, it should minimize the processing time. Otherwise there might be missed signals during the processing time.

In the four steps, when doing wavelet transform, signals with more detail and noise usually take longer time to process, which means it is essential to get rid of the obvious non-WRE signals before wavelet transform procedure. Therefore, the first two steps of PDR filtering should be robust enough to filter out as many non-WRE signals as possible, while passing all the WRE signals.

Although the computation of PDR in the pre-processing is very easy, the threshold of PDR used in the first round of filtration has a large impact on the computational complexity of the second round of analysis that involves wavelet transform. A higher PDR threshold reduces the computational demand of the wavelet process but may result in missed detection of the weak WRE signals. Fewer WRE signals will be miss-detected but the processing becomes more complex if a lower PDR threshold is used. Different thresholds for hydrophone and accelerometers are used to produce the results presented in the following section. These thresholds are selected according to different practical requirement.

5.3 Results

In our experiment, over 5000 signals are tested to compare the miss alarm (MA) and false alarm (FA). Here MA represents a real WRE signal that is not detected; and FA represents a noise signal that is mis-detected as WRE signal. 6 groups of data are listed as bellow:

Table 2: Results of 6 tested groups

	1	2	3	4	5	6
Type	ACC	Hyd	ACC	Hyd	ACC	Hyd
Tested	41	28	89	269	517	756
Detected	38	28	11	15	66	2
Confirmed	41	28	3	14	3	0
MA	3	0	0	0	0	0
FA	0	0	8	1	63	2

In Table 2, the first two groups are all confirmed WRE signals for Accelerometer (ACC) and Hydrophone (Hyd), respectively. We can see that Hydrophone signals are all detected, while three Accelerometer signals are missed. When double checking the missed data, we figure out that one of them is too weak to be detected, and the other two have too many low frequency components. However, all of them satisfy at least one feature. While in real applications, these signals will be automatically considered as suspected-WRE, and subjected to further inspection.

The two groups in the middle are samples of observed data when certain AE event occurs.It can be seen that most of the signals are noise, and about 5% of the data are WRE signals. Also it is clear that the algorithm claimed above detected all the signals, and especially in Hydrophone case it works better.

The last two groups are real data from the same source as the middle groups. However, these are the data randomly picked from daily monitoring, and we can see that over 99% of them are noise. Due to different condition, we can see that for Hydrophone, 99.9% of the noise is excluded, while for Accelerometer, more false alarms happened because of looser criteria. Consequently, in industrial application the proposed algorithm and criteria will not only greatly reduce the labor work of manual detection that the company is now using, as it is such a tedious and biased work to discriminate signals using eyes and ears, but also hugely increase the accuracy of detection.

6 CONCLUSIONS

In this paper, the Morlet wavelet is used to extract the features of WRE signal in Pre-stressed Concrete Cylinder Pipes (PCCP). Compared with Short-Time Fourier transform, the Wavelet transform provides better signal detection due to its inherent ability to detect abrupt changes. Also from the experimental results we can see that wavelet transform is a robust technique in time-scale-frequency analysis. In summary, wavelet analysis is an efficient technique for AE signal processing, especially in extracting detailed features, and detecting signals under investigation.

7 ACKNOWLEDGEMENT

This work is partially supported by Ontario Center of Excellence (OCE), Pressure Pipe Inspection Company Ltd. (PPIC) under grant number RY-EE-M50196-07, and Ryerson University. Special thanks to Theresa R. Erskine at the Research Office of Ryerson University, who bridges our collaboration with PPIC.

REFERENCES

[1] J. F. Stulen and F. B. Kiefner, "Evaluation of acoustic emission monitoring of buried pipelines", IEEE Trans. Ultronics Symposium, vol. 90, pp. 898-903, 1982.

[2] J. R. Smith, G. V. Rao, and R. Gopal, "Acoustic monitoring for leak detection in pressurized water reactors", ASTM. Special Technical Publications, pp. 177-204, Jan 1979.

[3] K. Yoshida, H. Kawano, Y. Akematsu, and H. Nishino, "Frequency characteristics of acoustic emission waveforms during gas leak", The European Working Group on Acoustic Emission, 2004.

[4] V. V. Muravev, M. V. Muravev, and S. A. Bekher, "A novel technique of AE signal processing for upgrading the accuracy of flaw localization", Acoustic methods, Russian journal of nondestructive testing, vol. 38, no. 8, pp. 600-610, Aug. 2002.

[5] B. Frielander and B. Porat, "Detection of transient signals by Gabor representation", IEEE Trans. Acoustics, Speech and Signal Processing, vol. 37, no. 2, pp. 169-180, 1989.
[6] D. Gabor, "Theory of communication", IEEE Trans, Communications, vol. 93, pp. 424-441, 1996.
[7] "Evaluation and repair of the ullrich medium service transmission main", http://www.ctlgroup.com, 2007.
[8] T. Boczar and D. Zmarzly, "Application of wavelet analysis to acoustic emission pulses generated by partial discharges", IEEE Trans. Dielectics and Electrical Insulation, vol. 11, no. 3, June 2004.
[9] S. Mallat, "A wavlet tour of signal processing", Academic Press, 1998.
[10] G.Kaiser, "A Friendly Guide to Wavelets", Birkhauser, 1994.
[11] C. Torrence and G. P. Compo, "A practical guide to wavelet analysis", Bulletin of the American Meteorological Society, vol. 79, no. 1, Jan. 1998.
[12] M. Frage, "Wavelet transforms and their applications to turbulence", Annu. Rev. Fluid Mech., vol. 24, pp. 395-457, 1992.
[13] C. Valens, "A really friendly guide to wavelets", https://www.cs.unm.edu/~williams/cs530/arfgtw.pdf. 1999.
[14] H. G. Stark, "Wavelets and signal processing", Springer, 2005.

Better testing... better products.

The Blachford Acoustics Laboratory

Bringing you superior acoustical products from the most advanced testing facilities available.

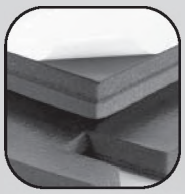

Our newest resource offers an unprecedented means of better understanding acoustical make-up and the impact of noise sources. The result? Better differentiation and value-added products for our customers.

Blachford Acoustics Laboratory features

- Hemi-anechoic room and dynamometer for testing heavy trucks and large vehicles or machines.
- Reverberation room for the testing of acoustical materials and components in one place.
- Jury room for sound quality development.

Blachford acoustical products

- Design and production of simple and complex laminates in various shapes, thicknesses and weights.
- Provide customers with everything from custom-engineered rolls and diecuts to molded and cast-in-place materials.

Blachford QS 9000 REGISTERED

www.blachford.com | Ontario 905.823.3200 | Illinois 630.231.8300